Grazing Collisions of Black Holes via the Excision of Singularities

Steve Brandt,[1] Randall Correll,[2,3] Roberto Gómez,[4] Mijan Huq,[1] Pablo Laguna,[1] Luis Lehner,[2,5] Pedro Marronetti,[2] Richard A. Matzner,[2] David Neilsen,[2] Jorge Pullin,[1] Erik Schnetter,[1] Deirdre Shoemaker,[1] and Jeffrey Winicour[4]

[1]*Center for Gravitational Physics and Geometry, Penn State University, University Park, Pennsylvania 16802*

[2]*Center for Relativity, The University of Texas at Austin, Austin, Texas 78712*

[3]*National Aeronautics and Space Administration, Washington, D.C. 20546*

[4]*Department of Physics and Astronomy, University of Pittsburgh, Pittsburgh, Pennsylvania 15260*

[5]*Department of Physics and Astronomy, The University of British Columbia, Vancouver, British Columbia, Canada V6T 1Z1*

(Received 15 August 2000; revised manuscript received 15 September 2000)

We present the first simulations of non-head-on (grazing) collisions of binary black holes in which the singularities are excised from the simulation. Initially equal mass m black holes (spinning or not) are separated by $\approx 10m$ and with impact parameter $\approx 2m$. Evolutions to $t \approx 35m$ are obtained where two separate horizons are present for $t \approx 3.8m$; then a single enveloping horizon forms indicating that the holes merged. Apparent horizon area estimates suggest gravitational radiation of about 2%–3% of the total mass. The evolutions end after a moderate amount of time because of instabilities.

PACS numbers: 04.25.Dm, 04.30.Db, 97.60.Lf

Introduction.— Gravitational wave detectors [1] will soon begin searching for gravitational radiation from astrophysical binary compact objects. To understand these observations, and to predict parameter regimes in which to search for their radiation, efforts are underway to model the interaction of compact sources. We report here a direct numerical simulation of interacting spinning *black hole* binaries, in genuinely hyperbolic (non-head-on) trajectories. The initial spin angular momenta evolved here are either zero or parallel to each other and perpendicular to the orbital plane. The interior of the equal mass holes and their interior singularities are excised from the computation. (Our method is *neither* restricted to equal masses *nor* to parallel spins.) Evolution is carried out in a *Cauchy* scheme, in which the state of the gravitational system (the three-spatial metric g_{ab}) and its rate of change (the three-spatial extrinsic curvature K_{ab}) are specified at one instant (i.e., on a three-dimensional spacelike hypersurface) and are then stepped to the next instant using an "Arnowitt-Deser-Misner" (ADM) [2] form of the Einstein evolution equations [3]. The evolution is unconstrained, and maintenance of the constraint functions with small error is verified throughout the run.

This work extends previous work on head-on encounters [4–7]. It is comparable to recent results of Brügmann [8]: non-head-on black hole evolution through to significant interaction and merger. But our approach has a novel feature: the *singularity-excising* character of the computation of generic encounters which allows "natural" motion of the black holes through the computational grid. Singularity excision may be crucial to carrying out long term simulations predicting gravitational waveforms through several wave cycles. Considerable efforts are being invested on finding the best possible way(s) to implement this strategy in 3D [9].

Initial data.—We carry out three binary black hole simulations. Data are created with *spinning* holes, each of mass m, located at $(\pm 5m, \pm m, 0)$, each with Kerr spin parameter a. The holes are boosted in opposite $\hat{\mathbf{x}}$ directions with speed $c/2$, representing a grazing collision with impact parameter of $2m$ (and resulting total orbital angular momentum in the $\hat{\mathbf{z}}$ direction). We distinguish three cases: case (I)—both holes have $a = 0.5m$ opposite to the orbital angular momentum, case (II)—nonspinning holes $a = 0$, and case (III)—both holes have $a = 0.5m$ aligned with the total angular momentum.

The total initial ADM mass of each simulation is $2.31m$, which agrees very well with the estimate given by the special relativistic limit $m_{\rm ADM} = 2\gamma m$, with $\gamma = (1 - 0.5^2)^{-1/2} = 1.155$. The total initial ADM angular momentum $\mathbf{J} = J\hat{\mathbf{z}}$ is 0.0, $1.17m^2$, and $2.34m^2$ for cases I, II, and III, respectively (see [10]).

The data setting technique is based on the boost-invariant Kerr-Schild [11] form of the Kerr black hole metric. Our *Cauchy* formulation requires first the solution of the initial data problem. As outlined in [12–14], superposed boosted Kerr-Schild data for two single holes produce a conformal background space; the physical data are solved via a York-conformal approach (solving four coupled elliptic equations) [15] on this background. Note that even when an exact solution of the elliptic equations is known, the error in the evolved solution will be determined by the inherent evolution-equation truncation error. Therefore, the accuracy of the elliptic solver employed need be consistent just with this truncation error. For the discretization used here ($\Delta x = m/4$) the truncation error is of order 5%. The quality of the data is validated by computing the constraints, normalized to a dimensionless quantity by the factor m^{-2}. Analytically the constraints should be zero everywhere. In fact, with the parameters of the problem, and with the current discretization and truncation error, the superposed background solution is acceptable with no further elliptic problem solution [14] (i.e., the zeroth order of the elliptic solver). However,

 0031-9007/00/85(26)/5496(4)$15.00

as we progress to larger and better resolved evolutions, we find it mandatory to cycle through the elliptic solve step [16] to obtain satisfactory solution of the constraints. Figure 1 presents the Hamiltonian constraint for case III, evaluated at integration time step $t = 3m$ along the $\hat{\mathbf{x}}$ axis, together with a time history of the l_2 norm (over volume outside the horizons, and excluding the outer boundary region) of the Hamiltonian constraint and the similarly normed momentum constraint. The late time rise in the momentum constraint in Fig. 1 shows the beginning of the exponential mode that appears at about $t = 36m$ and ends the simulation. We have quite good constraint behavior, of order 0.4%, with peak errors in the Hamiltonian of order 5% until that time.

Evolution methods.—The time evolutions presented here are done using AGAVE, a code that solves the Einstein equations in an ADM 3 + 1 form via finite difference techniques [3]. A parallel implementation is obtained with the use of MPI [17], employing the Cactus computational toolkit [18] solely to aid in this task. AGAVE is a major revision of the binary black hole grand challenge alliance Cauchy code [19,20]. The *lapse* function α and *shift* vector β^i express coordinate conditions which are chosen to allow the black holes to move freely. For our simulations, *prior* to the time that a single black hole surrounding the incoming pair is detected, we use a superposition of functions from boosted black holes: $\alpha = \alpha_1 + \alpha_2 - 1, \beta^i = \beta_1^i + \beta_2^i$, where these functions are centered with the current location of the holes,

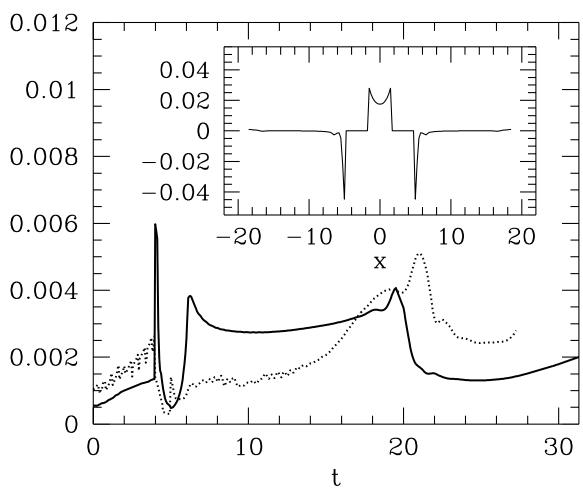

FIG. 1. For case I (and grid±20), the Hamiltonian and momentum constraints, on the domain of outer communication [outside the apparent horizon(s) and inside the outer boundary blending zone]. We give the time history of the l_2 (rms) norm of the Hamiltonian (solid line) and the l_2 norm over all three components of the momentum constraint (dotted line). The momentum l_2 is constructed only along coordinate lines (all that is available from this computation); the Hamiltonian l_2 is computed from the whole volume. The sudden change in the errors at $t \approx 4m$ occurs when a single outer apparent horizon envelops the merging holes. Also, the drop at $t \approx 20m$ is due to boundary effects. The inset shows the Hamiltonian constraint along the x axis at time $t = 3m$.

and with the velocity initially obtained from Newtonian approximation to the trajectories of the holes and subsequently inferred from the history of the locations of the apparent horizons (see below); *after* the detected merger, we use the lapse and shift of a single black hole with a mass, which is the sum of the original bare masses, and angular momentum, which is the (naive vectorial) sum of the spin and orbital angular momentum in the original system. (See *Discussion* below.)

The interior of the black holes is excised (Unruh, quoted in [21]). We use the apparent horizon surface, locatable at each time slice, as a marker for the excision. We utilize a combination of two different finite difference methods to find the apparent horizon: a direct solver [22] and a curvature flow method [23]. Once the apparent horizon is located, we define a *mask* function that delineates the excluded region (interior to the holes) from the computation. The result is that we literally evolve two holes moving freely through the computational domain. That domain is a 161^3 lattice, corresponding at our resolution to a cube $(40m)^3$ ($\pm 20m$ in each direction from the centered origin). However, boundary conditions are set by providing Dirichlet boundary conditions for g_{ab} and blending [24,25] outwards from a sphere of radius $19m$ the computational solution of K_{ab} to an analytically given (time-dependent) solution for K_{ab} at the outer boundary sphere. "Blending" means taking a linear combination of values from the computed and the analytically given solution, over a few (here, four) spatial zones, reducing gradients and second derivatives at the boundary. The analytic blending solution is created by superposition of boosted holes given by the initial data construction (with centers and velocities propagated according to the lapse and shift computation) or after the merger by the final estimated black hole with postmerger lapse and shift.

The discretization of the Einstein equations is consistent to second order accuracy. On the time scale where instabilities do not play a significant role, the convergence rate of this code is ≈ 1.6, reduced from 2 apparently because of extrapolation at the excision boundaries.

Results.—To the current accuracy of the code, cases I–III behave similarly. The total proper area of the apparent horizon A for case I is shown in Fig. 2. The value of A is particularly interesting since it provides a measure of the total mass contained in the apparent horizon. For a given black hole of mass m and spin parameter a its area is $A_{\mathrm{BH}} = 4\pi(R_+^2 + a^2)$ (with $R_+ = m + \sqrt{m^2 - a^2}$). Since at early times there is no common apparent horizon the total area is approximately $A \approx A_{\mathrm{BH1}} + A_{\mathrm{BH2}} = 2A_{\mathrm{BH1}}$, as the holes merge the total mass enclosed in the common horizon is (roughly) expected to double, and hence its area would be 4 times as big, i.e., for a nonspinning final black hole $A \approx 4\pi[2(2m)]^2 \lesssim 4A_{\mathrm{BH1}}$. Therefore, a plot of A vs time (like the one in Fig. 2) shows a considerable "jump" at the time the holes merge $t \approx 3.8m$. Additionally, effects of the outer boundary can be clearly seen in Fig. 2. For a ± 10 grid an abrupt "kink" is seen

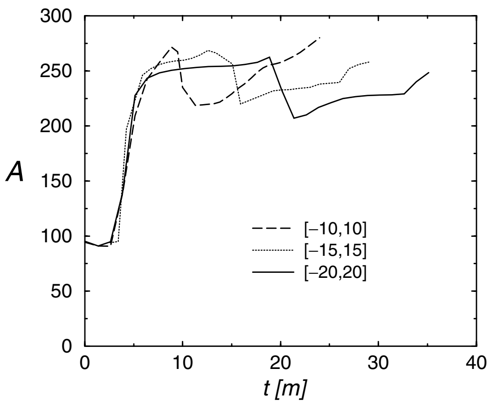

FIG. 2. The area of the apparent horizon(s) (transition to a single horizon at $t \approx 4m$) for case I (spatial resolution $\Delta = M/4$). For the smallest domain ($\pm 10m$, dashed line) the simulation runs to $t \approx 26m$ and exhibits strong boundary effects at $t \approx 9m$. For the $\pm 10m$ domain (dotted line), the simulation runs to $t \approx 31m$ exhibiting boundary effects at $t \approx 14m$. In the larger ($\pm 20m$) domain (solid line) boundary effects show at later time, around $19m$. Instabilities cause the measured area to rise abruptly at $t \approx 36m$ and eventually stop the simulation.

at $t \approx 9m$ while in the ± 20 grid the kink appears at $t \approx 19m$. At about $t \approx 36m$ ($t \approx 26m$) apparent instabilities in the $\pm 20m$ ($\pm 10m$) grid cause a rapid increase in the computed horizon size and eventually crash the run. Thus at $t \approx 35m$ the solution becomes untrustworthy. While the simulation is free of boundary effects the coincidence of the measured horizon area values supports confidence in the results. Figures 3A–3F track the apparent horizons through the merger for case I. A single enveloping black hole appears at $t \approx 3.8m$. The horizon oscillates and grows slightly.

We have in place Cauchy-characteristic extraction, where the Cauchy solution sampled at some "large" radius acts as data for a characteristic evolution to infinity [26,27] for waveform extraction. We also can compute the Newman-Penrose tensor ψ_4, which captures at null infinity the outgoing radiation. Additionally, we are developing a perturbative radiation extraction module. We are preparing a paper explaining how these tools are applied and illustrating the radiation patterns obtained from these simulations.

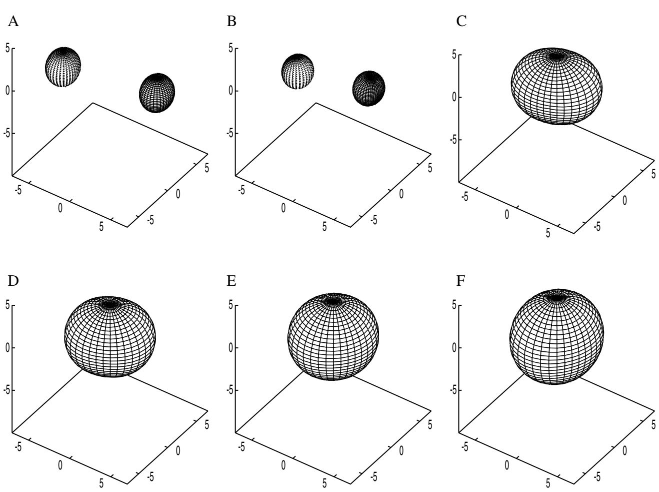

FIG. 3. For case I, time history of the horizons. The times corresponding to (A)–(F) are $t = 0$, $2.6m$, $5.1m$, $8.8m$, $13.8m$, and $18.8m$. These are coordinate plots; the corresponding areas appear in Fig. 2. After the merger the horizon oscillates through a fraction of a cycle.

Discussion and future directions.—The simulations reported here are genuinely, but not excessively, hyperbolic encounters. A Newtonian estimate gives a free fall velocity of $0.4c$ from infinity, as compared with the velocity $0.5c$ specified in our initial data. Future work will concentrate on generic hyperbolic and elliptic orbits.

Ongoing research concerns the late-time stability of the black hole simulations. We have carried out a number of one-dimensional simulations, all of which have longer term stability than this three-dimensional simulation of merged holes. We are investigating the behavior of the differencing scheme at the inner boundary. (The one we use behaves well in the spherical case.) We are implementing a new outer boundary algorithm which has been shown to be robustly stable in a linearized version of the code [28]. We are developing more sophisticated gauges based on elliptic equations for the lapse and the shift. These include the minimal distortion and minimal shear gauges [29] and other elliptic gauges [12,30]. Stable evolution of single black holes is quite sensitive to gauge conditions, and we anticipate much useful science from future improvement in the lifetime of our simulations of black hole mergers.

Our gauge and boundary conditions for the final merged black hole naively assume that all the initial mass (i.e., $M_{\rm final} = 2m$) and angular momentum reside in the final hole: $J_{\rm final} = a_{\rm final} \times M_{\rm final}$. For cases I, II, and III our gauge takes $a_{\rm final} = (0, 0.25, 0.5) \times M_{\rm final}$. These estimates do not take into account the emission of energy and angular momentum during the dynamics or the γ factor in the initial mass and angular momentum. The actual postcollision mass and angular momentum of the residual hole will be evaluated to further improve the simulations; behavior of the code is robust under changes in the final assumed mass and spin.

Of extreme interest is the size of the final apparent horizon. The *total* initial ADM mass leads to horizon area of $4\pi(2 \times 2.31m)^2 \approx 268m^2$. The postmerger numerically computed apparent horizon area (Fig. 2) is about $255m^2$, 5% smaller than this estimate. This measure would give a preliminary indication that total energy radiated in this simulation is about 2.6%. However, we have yet to complete a three-dimensional *event* horizon tracker, which will allow a correct comparison of the initial and final *event* horizon area.

The present work demonstrates the first simulation of binary black hole systems via the excision of singularities. The data sets evolved are not only useful for validation of the techniques employed here but as valid data sets in an astrophysical sense for the final "plunge" of the merger. In this work we (a) demonstrate well behaved (convergent) descriptions of the black holes as they evolve, (b) show that apparent horizon tracking and black hole excision can produce dynamical multiblack hole spacetimes, with reasonably well controlled errors for a considerable length of time (long enough for an accurate modeling of the merger phase), and (c) demonstrate that relatively unsophisticated gauge functions α and β can lead to physically interesting evolution lifetimes.

This work owes much to the Binary Black Hole Grand Challenge, and we thank all the members of that effort. This work was supported by NSF PHY/ASC 9318152 (ARPA supplemented), PHY 9310053, PHY 9800722, and PHY 9800725 to the University of Texas at Austin, PHY 9800973 and PHY 9800970 to Penn State University, and PHY 9510895, INT 9515257, and PHY 9800731 to the University of Pittsburgh. R. M. thanks the Observatoire de Paris, where some of this work was carried out, and Los Alamos National Laboratory for support during the initial stages of this research. E. S. acknowledges support from DAAD. Computations were carried out at the National Center for Supercomputing Applications, at the Albuquerque High Performance Computing Center, and at Los Alamos National Laboratory.

[1] LIGO: A. Abramovici *et al.,* Science **256**, 325 (1992); GEO: K. Danzmann and the GEO Team, Lect. Notes Phys. **410**, 184–209 (1992); VIRGO: C. Bradaschia *et al.,* Nucl. Instrum. Methods Phys. Res., Sect. A **289**, 518 (1990); TAMA: K. Tsubomo, M.-K. Fujimoto, and K. Kuroda, in *Proceedings of the TAMA International Workshop on Gravitational Wave Detection* (Universal Academic Press, Tokyo, Japan, 1996); LISA: *Proceedings of the First International LISA Symposium on Classical Quantum Gravity* [Classical Quantum Gravity **14**, 1397 (1996)].

[2] R. Arnowitt, S. Deser, and C. Misner, in *Gravitation—An Introduction to Current Research,* edited by L. Witten (Wiley, New York, 1962).

[3] Richard A. Matzner, in *Classical and Quantum Black Holes,* edited by P. Fre, V. Gorini, G. Magli, and U. Moschella (Institute of Physics Publishing, Bristol, 1999).

[4] S. G. Hahn and R. W. Lindquist, Ann. Phys. (N.Y.) **29**, 304 (1964).

[5] K. R. Eppley, Phys. Rev. D **16**, 1609 (1977).

[6] L. Smarr, in *Sources of Gravitational Radiation,* edited by L. Smarr (Cambridge University Press, Cambridge, England, 1978).

[7] P. Anninos *et al.,* Phys. Rev. Lett. **71**, 2851 (1993); P. Anninos *et al.,* Phys. Rev. D **52**, 2044 (1995); P. Anninos *et al.,* Phys. Rev. D **52**, 2059–2082 (1995).

[8] B. Brügmann, Int. J. Mod. Phys. D **8**, 85 (1999).

[9] L. Kidder *et al.,* Phys. Rev. D **62**, 084032 (2000); L. Lehner, M. Huq, and D. Garrison, Phys. Rev. D **62**, 084016 (2000); M. Alcubierre and B. Brügmann, gr-qc/0008067.

[10] Spatial components of angular momentum (e.g., spin) perpendicular to the motion transform with one power of γ and stay perpendicular to the motion. The orbital angular momentum $\mathbf{L} = \mathbf{r} \times \mathbf{p}$ also contains one power of γ in $\mathbf{p}$. Hence $\mathbf{J}$ contains one power of γ. See L. Landau and E. Lifshitz, *Classical Theory of Fields* (Pergamon Press, Oxford, 1962), revised 2nd ed., p. 46.

[11] R. P. Kerr and A. Schild, in *Applications of Nonlinear Partial Differential Equations in Mathematical Physics, Proceedings of the 17th Symposium in Applied Mathematics, New York, 1964* (American Mathematical Society, Providence, 1965); R. P. Kerr and A. Schild, in *Atti del Convegno Sulla Relatività Generale: Problemi Dell'Energia E Onde Gravitazionali, Firenze, 1964,* edited by G. Barbera (Comitato Nazionale per le Manifestazioni Celebrative, Roma, 1964).

[12] Richard A. Matzner, M. F. Huq, and D. Shoemaker, Phys. Rev. D **59**, 024015 (1999).

[13] R. Correll, Ph.D. thesis, The University of Texas, 1998.

[14] P. Marronetti *et al.,* Phys. Rev. D **62**, 024017 (2000).

[15] J. W. York and T. Piran, in *Spacetime and Geometry: The Alfred Schild Lectures,* edited by Richard A. Matzner and L. C. Shepley, (University of Texas Press, Austin, TX, 1982); G. B. Cook, Ph.D. dissertation, The University of North Carolina at Chapel Hill, 1990.

[16] P. Marronetti and R. A. Matzner, following Letter, Phys. Rev. Lett. **85**, 5500 (2000).

[17] See http://www.mpi-forum.org/

[18] See http://www.cactuscode.org/

[19] The Binary Black Hole Grand Challenge Alliance, G. Cook *et al.,* Phys. Rev. Lett. **80**, 2512 (1998).

[20] M. Huq and Richard A. Matzner (to be published).

[21] J. Thornburg, Classical Quantum Gravity **4**, 1119 (1987).

[22] M. F. Huq, M. W. Choptuik, and Richard A. Matzner (to be published).

[23] D. Shoemaker, Ph.D. dissertation, The University of Texas, 1999; D. Shoemaker, M. Huq, and Richard A. Matzner, Phys. Rev. D (to be published).

[24] R. Gomez, in Proceedings of the Binary Black Hole Grand Challenge Workshop, Los Alamos, NM, 1997 (unpublished).

[25] The Binary Black Hole Grand Challenge Alliance, L. Rezzolla *et al.,* Phys. Rev. Lett. **80**, 1812 (1998); L. Rezzolla *et al.,* Phys. Rev. D **59**, 064001 (1999).

[26] N. T. Bishop *et al.,* in *Black Holes, Gravitational Radiation and the Universe,* edited by Bala Iyer and Biplab Bhawal (Kluwer, Dordrecht, The Netherlands, Boston, 1998).

[27] N. T. Bishop *et al.,* Phys. Rev. Lett. **76**, 4303 (1996).

[28] B. Szilagyi *et al.,* Phys. Rev. D **62**, 104006 (2000).

[29] L. Smarr and J. York, Phys. Rev. D **17**, 2529 (1978).

[30] P. Brady, J. Creighton, and K. Thorne, Phys. Rev. D **58**, 061501 (1998).